Sensing On-road Objects by Infrared Hyper Spectrum

Yukio KOSUGI*, Toru MURASE*, Taro ASANO, Kuniaki Uto, Shigenori TAKAGISHI
and Masahiro MORIGUCHI

Prevention of traffic accidents between human and vehicles on road has become one of the major issues today and the development of advanced in-vehicle safety systems is highly expected. A sensing system installed into a vehicle can be a solution to the issue, playing a complementary role for the elderly with poor detection capabilities, especially in aging society.
Although visible light imaging and thermal infrared ray (TIR) sensing have been put into practical use in some fields, yet they fall short of sensing accuracy due to their moisture-absorption property or susceptibility to other heat sources, such as vending machines.
Focusing on short wavelength infrared rays (SWIR), the authors have developed the basic technology of sensing and detecting objects by using hyper spectra. This paper presents an overview of the SWIR hyper spectrum sensing method and its evaluation system, along with the experimental results proving the method's high accuracy in human detection.

Keywords: hyper spectrum sensing, human detection, short-wave infrared

1. Introduction

Reducing the number of traffic accidents is one of the major challenges in Japan. In particular, as the number of elderly people increases, advanced auxiliary safety functions installed to vehicles are desired in order to compensate for aged pedestrians' lowering perception abilities. Take hybrid or electric automobiles for example. Their noiseless movement seems to be a great advantage in urban life, however, it can also increase the chance of traffic accidents related to pedestrians' unawareness of approaching vehicles. In addition, advanced electric wheelchairs for the physically disabled have also become risk factors for those pedestrians. To make urban life safer for both drivers and pedestrians, they should be provided with adequate information for risk aversion. In this regard, horns and other alarm systems mounted on vehicles can be a solution. And for such alarms to be used to the fullest, the vehicle must be equipped with a reliable function to detect pedestrians on the road. The systems for detecting and distinguishing pedestrians from other obstacles on the road often use feature extraction methods utilizing luminance histogram, rectangle feature quantity of visible light images, and the spatial distribution of the luminance value on two-dimensional (2D) images. The processing accuracy using support vector machine (SVM) is also being improved [(1)] for a better extraction.

A detection system using thermal infrared sensors has also been practically used. However, it has some problems as follows; the electromagnetic waves in the thermal region are absorbed by water, pedestrians can be overlooked when the temperature gradient between the pedestrian and his/her background is small, and other heat sources, such as vending machines, can be misidentified as a pedestrian.

In general, optical sensors used for remote sensing are classified as shown in **Table 1**, according to the band and wavelength. In this study, we focused on the short-wavelength infrared region (SWIR) to which less attention has been paid so far, and considered to make use of the SWIR based on the reflection spectral features of obstacles acquired by a hyperspectral sensor (HS sensor). Based on the spectral consideration on the HS observation data in the SWIR, we report on the development and design of the basic system to detect objects using reflection spectra.

2. Observation and Application of HS Images

The HS sensor is effectively used to examine the reflection characteristics of objects in an unknown wavelength region. The HS is an optical sensor used to detect the reflection spectral information of the objects by dividing the spectral range into continuously arranged narrow bands usually exceeding 100. In the field of remote sensing, HS sensors have found applications in various fields,

Table 1. Commonly used remote-sensing bands and the wavelengths

Band	Ultra violet	Visible	Near infrared	Short-wavelengh infrared	Middle-wavelengh infrared	Thermal infrared
Abbr.	UV	V	NIR	SWIR	MWIR	TIR
Wavelength	<400nm	400-760nm	0.7-1μm	1.0-2.5μm	3-5μm	8-14μm

such as in aircrafts and satellites to facilitate the comprehensive observation of the ground uses, resource mapping, and vegetation in agricultural and forestry fields. Although the boundary between the HS sensor and the multi spectral sensor (up to several dozen bands) is not clearly defined in terms of band number, the sensor that has a spectroscopic function to continuously acquire the information of the adjacent bands is called an HS sensor. The Airborne Visible/Infrared Imaging Spectrometer (AVRIS), an airborne HS sensor that has been used by NASA and the Jet Propulsion Laboratory of California Institute of Technology since 1987, has the longest history of the operation [2]. This sensor has 224 bands, covering the range from 380 to 2500 nm and allowing the ground resolution of 20 m with the swath width of 11 km from the altitude of 20 km. Meanwhile, as for the HS sensor of the satellite installation, Hyperion (band number = 210, ground resolution = 30 m, swath width = 7.5 km) installed on the satellite EO-1 has been operated since 2000. In Japan, the Earth Remote Sensing Data Analysis Center (ERSDAC) promotes "Hyper project [3]" to accelerate the development of HS data application technology, in view of the launch of the satellite equipped with the HS sensor in 2013. In this project, various observations by the HS sensors installed in aircrafts have been conducted, such as CASI (Itres Co., Canada) and AISA (Specim Co., Finland).

In our study, PGP(prism grating prism) based spectroscopic line sensors (Imspector-V10 and Imspector-N17, Specim Co) were mounted on the truck crane and the 2D HS image was acquired by mechanically scanning the object via the rotational movement of the crane arm. When it was difficult to acquire the images via the crane mounted sensor, we measured the average luminance spectrum in a viewing angle using a spectrometer (Field Spec 3). In both cases, the reflectance spectra of objects were calculated by the standard white reference.

HS data provides a clue to assess the physical and chemical properties of the object, because it possesses reflection characteristics corresponding to the light absorption and transmission properties of each wavelength from the object. In the HS observation, enormous image data (normally over 100 bands) are acquired, however, because there is considerable amount of redundancy among the near-by bands, the minimum number of required bands to assess the condition of a specific object is rather small. In some extreme cases, two wavelengths are enough to extract adequate information by manipulating their reflectivity values. Normalized Difference Vegetation Index (NDVI) is a numerical indicator that is widely used in the remote sensing field. This index is calculated by normalizing the sum of two reflectivity values: the lowering reflectivity (around 680 nm band, due to the chlorophyll's absorption), and the increasing reflectivity (at the near infrared area). This technique is useful for assessing the vegetation condition using excessive satellite images.

This kind of normalization index can also be used to extract the properties of various objects in the SWIR region by using the following equation, in which the reflectivity at the two wavelengths (λ_1 and λ_2) are defined as $R(\lambda_1)$ and $R(\lambda_2)$.

$$NDX = [R (\lambda_1) - R (\lambda_2)] / [R (\lambda_1) + R (\lambda_2)]$$

Some examples of indices proposed by Kosugi Laboratory of Tokyo Institute of Technology are shown in **Table 2**. The moisture content ratio is defined by the weight of water contained per unit weight of dry soil and approximate values of the moisture ratio from 0 to 60% are estimated by substituting λ_1= 1696 nm and λ_2= 1426 nm to the equation [4]. By substituting λ_1 = 1070 nm and λ_2 = 1550 nm to the same equation, we can define "Normalized Difference Human Index (NDHI)," which can extract human skin out of various kinds of background [5], [6], as shown in the example of **Photo 1**.

Two years later from our report above, the U.S. Air Force Research Laboratory [7] announced Normalized Difference Skin Index (NDSI), a normalized index that was defined by similar values to those of our report, λ_1 = 1100 nm and λ_2 = 1400 nm.

Table 2. Examples of normalized indices defined in SWIR region

Target	Abbr.	λ_1 (nm)	λ_2 (nm)
Soil moisture [4]	NDSMI	1696	1426
Human skin [5], [6]	NDHI	1070	1550
Oak wilt [8]	$NDWI_{swir}$	1460	1280

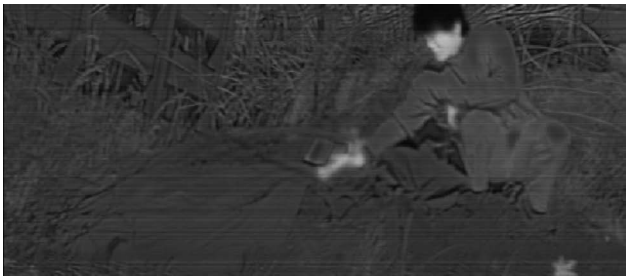

Photo 1. Human skin extracted by NDHI

This normalized index form is also applied to the assessment of the water stress in forests by substituting λ_1 = 1460 nm and λ_2 = 1280 nm. This Normalized Difference Water Index (NDWI) can greatly contribute to the detection of oak wilt infected trees, such as quercus serrata and quercus mongolica, along the coast of the Japan Sea.

However, these normalized indices usually use only two bands and the rest of the information is discarded without being used. To make the most of the information contained in the HS data, neural networks or other learning mechanisms need to be applied. Due to the redundancy in adjacent bands, some ten applicable bands are selected by Particle Swarm Optimization (PSO) or other optimization techniques [9]. In our study, however, sticking to the aim of developing the detecting technique of objects on the road, we placed the highest priority on the processing speed and limited the SWIR reflectance data up to five bands.

3. Spectral Profile of Obstacles on Road and its Discrimination Logic

The SWIR reflectance spectra of typical obstacles on the road are shown in **Fig. 1**. For the cases of (a) human skin, (b) vegetation and (c) animal/cloth, relatively high reflectance values are observed, whereas for inorganic matter, such as (d) car/ metal, (e) concrete and (f) asphalt, the spectral profiles are rather flat over the whole wavelength range. It is important to note that significant errors can be generated in the standard white reference due to the absorption by steam around 1380-1400 nm wavelength band, resulting in apparent increases in the reflectance variance.

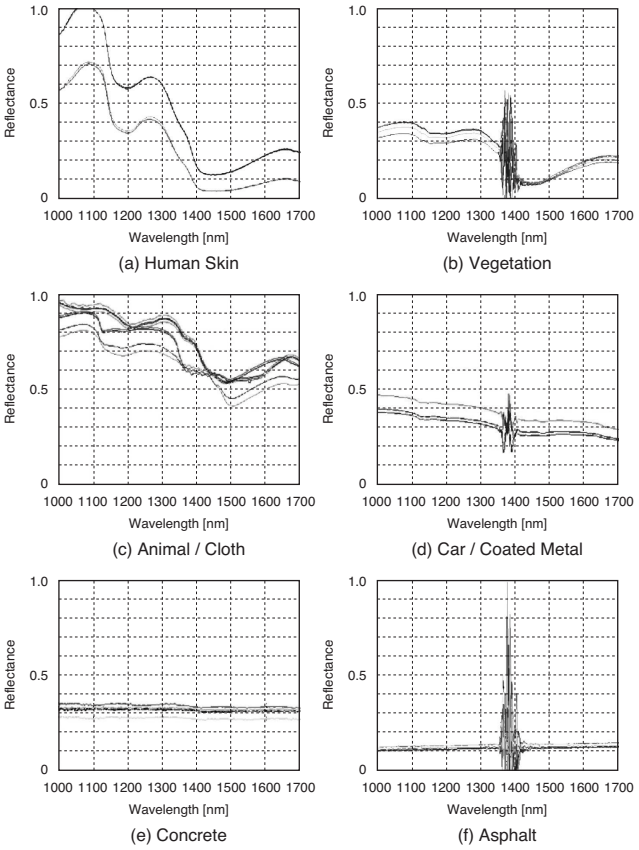

Fig. 1. SWIR reflectance spectral profile of typical obstacles on road

Excluding the unstable range above, we selected five bands suitable for the recognition of objects: 1100, 1200, 1300, 1500 and 1600 nm. Based on a spectral database derived from the observations of various objects, we designed decision tree logic for fast calculation. The processing flow of the logic is shown in **Fig. 2**.

In the processing system of **Fig. 2**, the objects' luminance value that is normalized by the standard white reference is input. First, in the comparative operation ①, the reflectance value at each band is compared with the predetermined threshold 0.02, and if all the reflectance values are 0.02 or smaller, then the object is determined as a car window. At the comparator ②, the polarity of "der 1 x (ND5 + ND3)" is determined by the computational decisions using the secondary difference calculated with three bands (1100, 1300 and 1500 nm) and normalized indices (ND3 and ND5) defined in the caption of **Fig. 2**. Similarly, in the following, concrete, asphalt, animal/cloth, vegetation and human skin are identified according to the polarity of the normalized calculation results. We carried out the aforementioned operation with 318 subjects to evaluate this logic and figure out its error rate. The con-

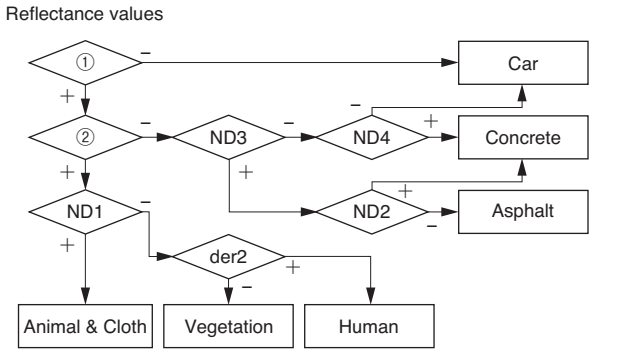

① the reflectance value at each band is compared with threshold 0.02. If all the reflectance values are 0.02 or smaller, the object is classified as the window glass of a car.
② judging polarity of der 1 x (ND5 + ND3)
der1: secondary difference calculated from R1200, R1300, R1500
der2: secondary difference calculated from R1100, R1200, R1500
ND1: (R1500-R1200) / (R1500+R1200)
ND2: (R1300-R1200) / (R1300+R1200)
ND3: (R1600-R1300) / (R1600+R1300)
ND4: (R1300-R1100) / (R1300+R1100)
ND5: (R1500-R1300) / (R1500+R1300)
* R1100 is the reflectance value at 1100 nm. Same expressions are used for R1200, R1300, R1500 and R1600.

Fig. 2. Object classification logic using five bands

Table 3. Confusion matrix for discrimination result using five bands

Classified Data	Reference Data Hum	Veg.	Ani.	Car	Asp.	Con.	Row Total	User's Accuracy
Human skin	48						48	100%
Vegetation		20					20	100%
Animal/Cloth		2	103				105	98.1%
Car/Metal				34		3	37	91.9%
Asphalt					48	2	50	96.0%
Concrete					5	53	58	91.4%
Column Total	48	22	103	34	53	58	318	
Producer's Accuracy	100%	91.0%	100%	100%	90.6%	91.4%	(306/318)= 96.2%	
	Overall Accuracy							

fusion matrix is shown in **Table 3**. For example, producer's accuracy in the table means that when 22 vegetation samples were tested, the classifier sorted 91.3 % right and misidentified the remaining 8.7% as animal/cloth. Meanwhile, user's accuracy states that out of all unknown samples that the classifier on site had classified as asphalt, 96% were actually asphalt and 4% were concrete.

Although the producer's accuracy and user's accuracy were not so high in the classification of concrete and asphalt samples, the producer's accuracy of human skin and automobile samples reached100%.

4. Testing Observation Apparatus

For obtaining 2D HS images, two methods are often used. One is the push broom method, in which an object is mechanically scanned with a line sensor, and the other is a method of using tunable optical filters placed on the 2D array of sensors. However, the scanning time of both methods can not be ignored for the fast observation. As stated in the previous section, human subjects and vehicles were identified with a high accuracy, despite the fact that we had selected only five bands of spectral data. Therefore we decided to construct a fast observation system capable of obtaining five bands of line images.

The optical parts of the HS sensor are shown in **Photo 2**. In this sensor system, parallel process is carried out for 128 image components (2 lines of 64 components). The monitoring result of the image preprocessing is shown in **Photo 3**. In this process, the horizontal position of the object is divided into 10 sections and projected on to the corresponding parts of the display. In the vertical direction, the average spectral intensity of each five band is indicated both in number and gray value.

As shown above, the intensity matrix data is processed by the quick classification logic of **Fig. 2**. The output of the logic is shown as a binary image, as seen in **Photo 4 (a)**, indicating the presence of cloths and human skin in the corresponding horizontal segment. This system completed all the processes within 1/30 seconds, corresponding to the TV frame rate, and is capable of real-time processing.

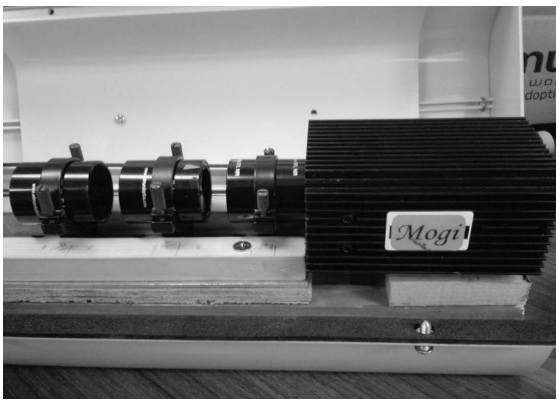

Photo 2. Optical parts of the sensor

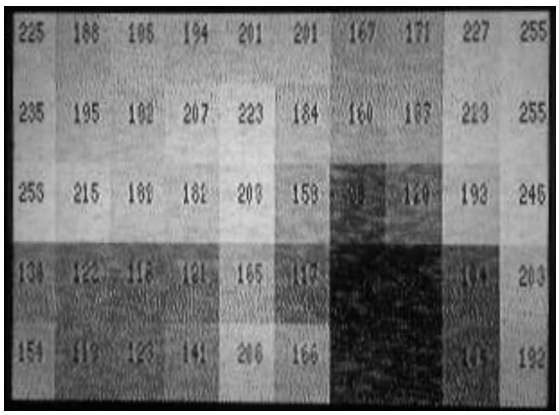

Horizontal axis: Object's horizontal position
Vertical axis: 255 x reflectance at each band

Photo 3. Preprocessing image

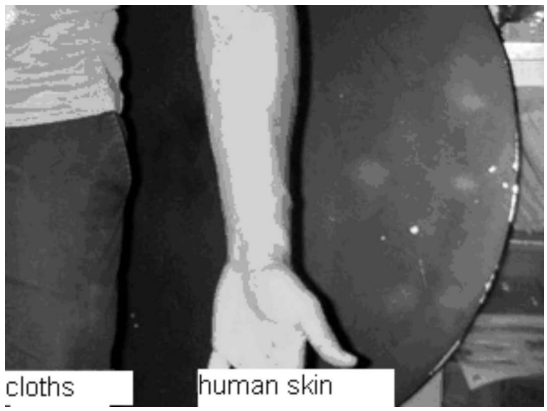

(a)

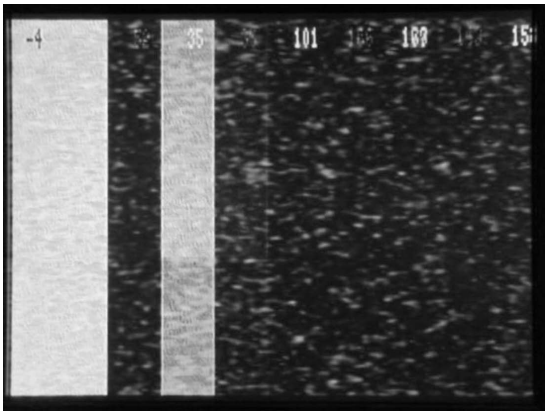

(b)

Photo 4. Real time detection of cloths and human skin
(a) RGB view of object (b) Detection result

5. Conclusion

I this paper, we described the possibility of detecting pedestrians out of other objects on the road by manipulating five spectral components in a short wavelength infrared

region, based on the fundamental mechanisms using hyperspectral database. We proposed a multi spectral line camera equipped with the logic of object classification and realized real-time obstacle detection using an SIMD type processing unit. Since this developed model acquires no 2D images of the road, individual privacy will be protected even from a low angle including electric wheelchairs.

Thus far, less attention has been given to the use of short wavelength infrared observation. This is partly because inexpensive silicon sensors could not cover the long wavelength and producing such semiconductor devices was thought to be unrealistic. As the III-V compound semiconductor technologies progress, sensing technology using the short wavelength infrared region will further advance in the future.

References

(1) Masakatsu Higashikubo, Takio Kurita, Development of Image Processing Sensors for Cooperative Driving Society Support Systems, SEI Technical Review, Vol.175, pp.108-112 (2009)

(2) NASA & Caltech Jet Propulsion Laboratory, AVRIS http://aviris.jpl.nasa.gov/

(3) Earth Remote Sensing Data Analysis Center: "Hyper Project" http://www.ersdac.or.jp/HYPER/index.html

(4) Masanori Fukusumi, Yohei Minekawa, Kuniaki Uto, Naoko Kosaka, Yukio Kosugi, Kunio Oda, Genya Saito: Optimization of Inter-Band Manipulation for the Soil Moisture Estimation Using Hyperspectral Data; Proc. 2006-fall Workshop of Japanese Agricultural Systems Society, pp.48-49 (2006)

(5) Takayuki Edanaga, Kuniaki Uto, Yukio Kosugi: "Research on the Human-Part Extraction using Short Wave Infrared Spectral Information"; Proc. 2005 fall Scientific Lectures of the Japan Society of Photogrammetry and Remote Sensing (2005)

(6) Takayuki Edanaga, Kuniaki Uto, Yukio Kosugi: "Research on the Human-Part Extraction using Short Wave Infrared Spectral Information," Journal of the Japan Society of Photogrammetry and Remote Sensing, Vol.46, No.2, pp.17-26 (2007)

(7) Abel S. Nunez and Michael J. Mendenhall, "Detection of Human Skin in Near Infrared Hyperspectral Imagery," vol. II, pp.621-624, Proc. IGARSS 2008 (2008)

(8) Yukio Kosugi, Kuniaki Uto, Taro Asano, Nobuki Kikuchi, Toshinari Ogata, Shinya Odagawa, Kunio Oda: Aerial Hyperspectral-Observation and Analysis of Japanese Oak Wilt, Proc. The Japan Forest SocietyCongress, Vol.120, p.283 (2009)

(9) Takayuki Edanaga, Yohei Minekawa, Sildomar T. Monteiro and Yukio Kosugi: "Studies on human skin extraction from hyperspectral data using particle swarm optimization," Journal of the Japan Society of Photogrammetry and Remote Sensing, Vol.47, No.3, pp.23-36 (2008)

(10) Taro Asano, Yukio Kosugi,kuniaki Uto, Tohru Murase, Goro Sasaki, Masahiro Moriguchi: Fundamental Consideration on the Recognition of Obstacles on The Road by using Infrared Hyperspectral Information, Proc. 2009 Annual Scientific Lectures of the Japan Society of Photogrammetry and Remote Sensing, pp.65-68(2009)

(11) Taro Asano, Yukio Kosugi, Kuniaki Uto, Toru Murase, Toro Sasaki and Masahiro Moriguchi: "Discrimination of Obstacles on the Road Using Hyper-spectral Dada," Proc. ACRS (Beijing 2009)

(12) Yoshihiro Fujita, Nobuyuki Yamashita, and Shinichiro Okazaki: "IMAP: Integrated Memory Array Processor – Toward a GIPS Order SIMD Processing LSI-," IEICE Trans. Electron, Vol. E76-C, No.7, pp.1144-1150 (1993)

Contributors (The lead author is indicated by an asterisk (*)).

Y. KOSUGI*

- Dr. of Eng.,
  Professor, Dept. of Mechano-Micro Eng., Interdisciplinary Graduate School and Engineering, Tokyo Institute of Technology
  His research interests include information processing in the nervous system and neural network-aided image processing in the medical and remote sensing fields.
  Member of IEEE, the Institute of Electronics, and the Japan Society of Photogrammetry and Remote Sensing.

T. MURASE*

- Ph.D.,
  Chief Engineer, Materials and Process Technology R&D Unit
  Chief Engineer, Information and Communications Technology R&D Unit
  Leader of Security, Safety and Ubiquitous NW WG
  He was a visiting fellow at Stanford University and Carnegie Mellon University.
  Member of ISCIE and IEICE.

T. ASANO

- Master's student, Interdisciplinary Graduate School and Engineering, Tokyo Institute of Technology

K. UTO

- Dr. of Eng.,
  Assistant Professor, Interdisciplinary Graduate School and Engineering, Tokyo Institute of Technology

S. TAKAGISHI

- Dr. of Eng.,
  Senior Assistant General Manager, R&D General Planning Division, Planning Department

M. MORIGUCHI

- Assistant General Manager, R&D General Planning Division, Planning Department